

# **EE568 – Selected Topics on Electrical Machines**

Project #1: Torque in a Variable Reluctance Machine

by

Hakan Saraç - 2408086

## 1. Table of Contents

2.	Introduction.....	2
3.	Question 1: Analytical Modeling .....	3
3.1.	Reluctance as a function of angle derivation .....	3
3.2.	Resultant torque.....	5
3.3.	Further improvements on analytical model.....	5
4.	Question 2: FEA Modeling (2D - Linear Materials).....	6
4.1.	Flux density distributions at rotor angle $0^\circ - 45^\circ - 90^\circ$ .....	6
4.2.	Inductance and stored energy at rotor angle $0^\circ - 45^\circ - 90^\circ$ .....	6
4.3.	Analytical results and FEA results comparison.....	8
5.	Question 3: FEA Modeling (2D - Nonlinear Materials).....	9
5.1.	Flux density distributions at rotor angle $0^\circ - 45^\circ - 90^\circ$ .....	9
5.2.	Inductance and stored energy at rotor angle $0^\circ - 45^\circ - 90^\circ$ .....	12
5.3.	Analytical results and FEA results comparison.....	12
6.	Question 4: Control Method .....	13
7.	Question 5: Motion Animation.....	13
8.	References .....	13

## 2. Introduction

In this project, characteristics of a simple electrical machine will be analyzed. The analysis procedure has started with analytical calculation assuming ideal conditions, such as assuming ideal materials, homogeneous flux distribution etc. After obtaining torque and inductance values using analytical results, ANSYS Maxwell is used as FEA tool is used for verification. Using ANSYS Maxwell, first a material with linear permeability and no saturation limit is used, then the results are compared with a material which has a nonlinear permeability and saturation limit.

The aspects of the electrical machine are provided in Figure 1. It is aimed to observe the flux density, torque, inductance reluctance etc. variation with the rotational part position.

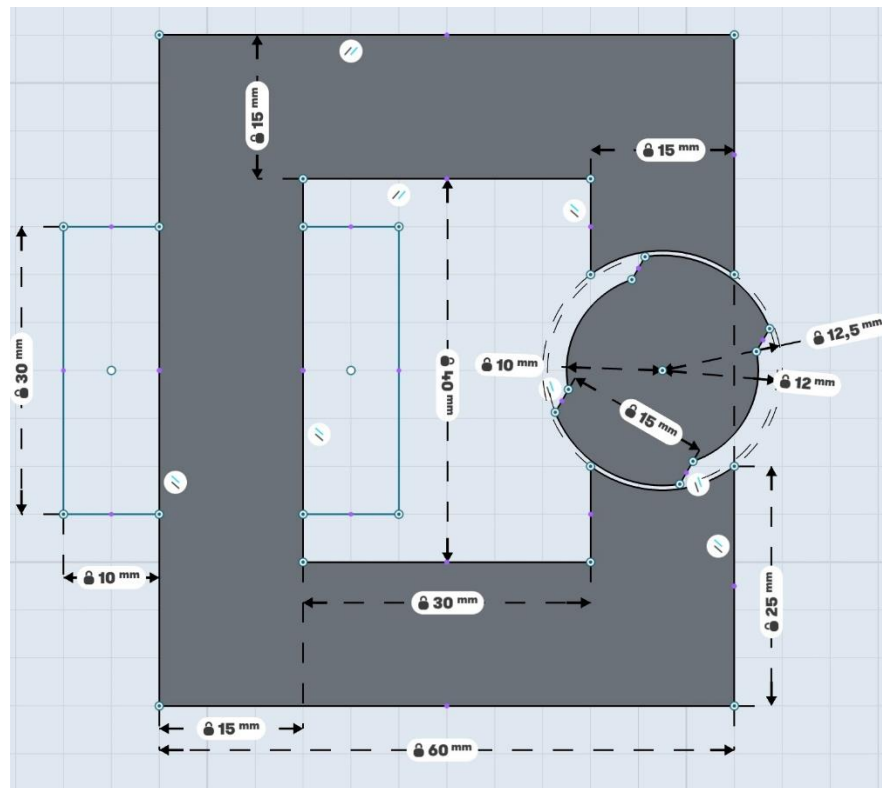


Figure 1: Machine 2D Drawing [1]

Other specifications of the machine are listed as:

- Coils are wound within 30mmx10mm rectangle areas
- Each airgap clearance is 0.5mm
- Depth of the core is 20mm
- Number of turns = 250
- Coil Current = 3 A DC

### 3. Question 1: Analytical Modeling

#### 3.1. Reluctance as a function of angle derivation

In order to simplify the analytical calculations, the dependency of the reluctance (and therefore inductance) with the rotor position is derived by assuming that the flux is flowing through either the 12mm radius part and/or 10mm radius part. The flux flowing through the linear part is ignored for this part. The flux flow assumption is shown more clearly in Figure 2. Moreover, the core is taken to be infinitely permeable and the fringing effects are neglected.

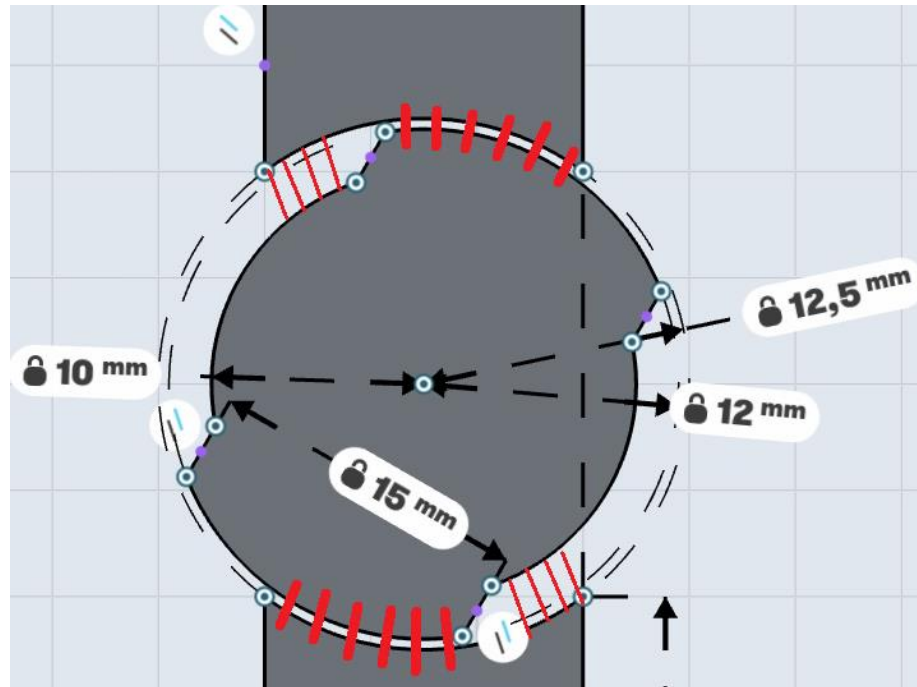


Figure 2: Flux path assumptions for analytical calculations (shown in red)

These assumptions led to simple expressions for the reluctance seen by the source. Three formulas are derived for  $0^\circ$ - $77.36^\circ$ ,  $77.36^\circ$ - $102.64^\circ$ ,  $102.64^\circ$ - $180^\circ$  degree regions. The positions at these angles are provided in Figure 3.

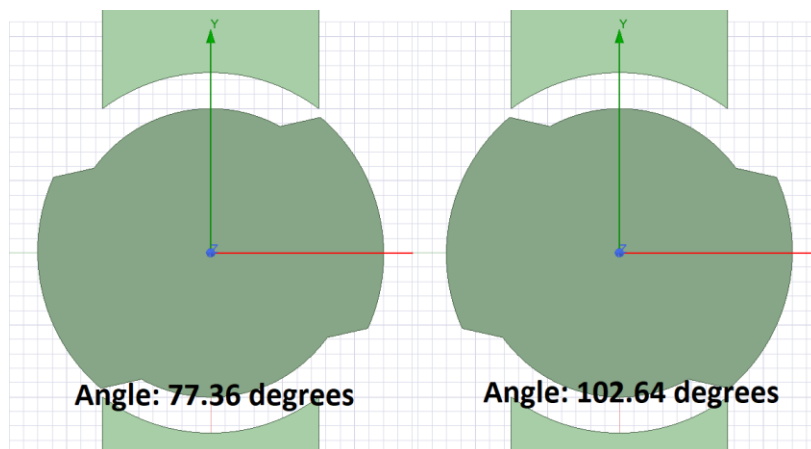


Figure 3: Rotor positions at critical angles

In part 1 angle is between 0°-77.36° degrees, the flux shared between two radial parts. During the reluctance calculations in this region, there assumed to be two parallel reluctance for flux path. The derived formulas are given in (1) & (2) and the resultant equivalent reluctance is given in (3).

$$R_{12mm\_part1} = \frac{l_{12mm}}{\mu_0 A_{12mm}} = \frac{0.5*10^{-3}*2}{\mu_0 * \frac{(77.36^\circ - \theta)}{360^\circ} * 2\pi * 12*10^{-3} * 20*10^{-3}} = 527714 * \left( \frac{360^\circ}{(77.36^\circ - \theta)} \right) \left( \frac{1}{Henry} \right) \quad (1)$$

$$R_{10mm\_part1} = \frac{l_{10mm}}{\mu_0 A_{10mm}} = \frac{2.5*10^{-3}*2}{\mu_0 * \frac{\theta}{360^\circ} * 2\pi * 12*10^{-3} * 20*10^{-3}} = 3166286 * \left( \frac{360^\circ}{\theta} \right) \left( \frac{1}{Henry} \right) \quad (2)$$

$$R_{eq\_part1} = \frac{R_{12mm\_part1} * R_{10mm\_part1}}{R_{12mm\_part1} + R_{10mm\_part1}} \left( \frac{1}{Henry} \right) \quad (3)$$

In part 2, the angle is between 77.36°-102.64° degrees, all the flux is assumed to be flowing through the 10mm radius part and reluctance does not change with the position. The resultant reluctance is provided in (4).

$$R_{eq\_part2} = R_{10mm\_part2} = \frac{l_{10mm}}{\mu_0 A_{10mm}} = \frac{2.5*10^{-3}*2}{\mu_0 * \frac{77.36^\circ}{360^\circ} * 2\pi * 12*10^{-3} * 20*10^{-3}} = 14734531 \left( \frac{1}{Henry} \right) \quad (4)$$

In part 3, the angle is between 102.64°-180° degrees, similar to the part 1, the flux is shared between two radial parts. The derived formulas are given in (5) & (6) and the resultant equivalent reluctance is given in (7).

$$R_{12mm\_part3} = \frac{l_{12mm}}{\mu_0 A_{12mm}} = \frac{0.5*10^{-3}*2}{\mu_0 * \frac{(\theta - 102.64^\circ)}{360^\circ} * 2\pi * 12*10^{-3} * 20*10^{-3}} = 527714 * \left( \frac{360^\circ}{(\theta - 102.64^\circ)} \right) \left( \frac{1}{Henry} \right) \quad (5)$$

$$R_{10mm\_part3} = \frac{l_{10mm}}{\mu_0 A_{10mm}} = \frac{2.5*10^{-3}*2}{\mu_0 * \frac{(180^\circ - \theta)}{360^\circ} * 2\pi * 12*10^{-3} * 20*10^{-3}} = 3166286 * \left( \frac{360^\circ}{(180^\circ - \theta)} \right) \left( \frac{1}{Henry} \right) \quad (6)$$

$$R_{eq\_part3} = \frac{R_{12mm\_part3} * R_{10mm\_part3}}{R_{12mm\_part3} + R_{10mm\_part3}} \left( \frac{1}{Henry} \right) \quad (7)$$

### 3.2. Resultant torque

The resultant reluctance, inductance and torque versus mechanical angle due to the calculations provided in 3.1. are provided in Figure 4 for a constant DC excitation. The torque is derived due to the variation of inductance with the mechanical angle.

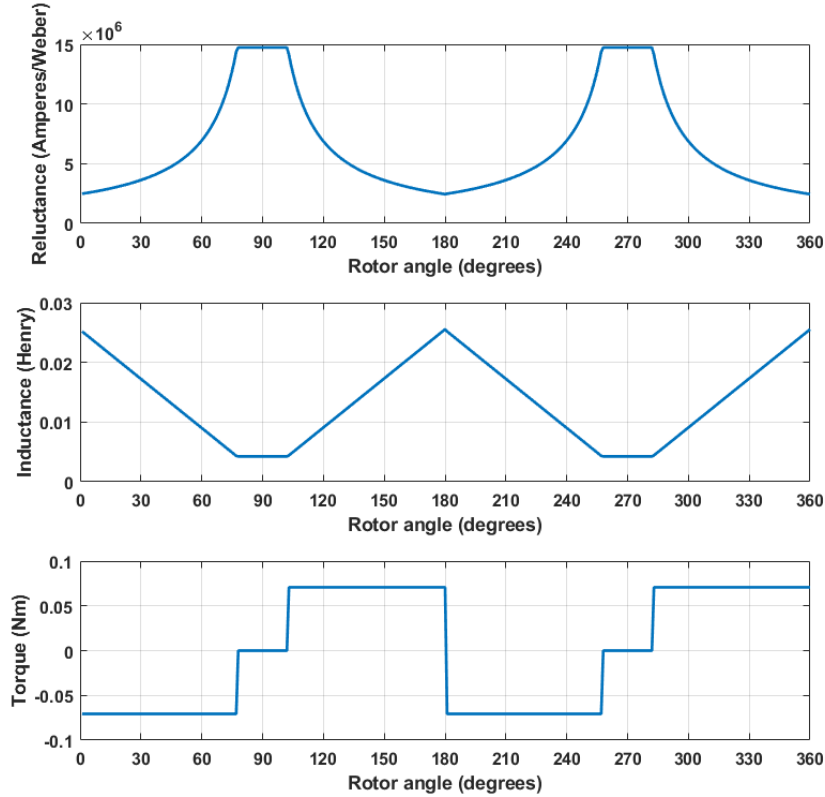


Figure 4: Reluctance, inductance and torque vs angle graphs

### 3.3. Further improvements on analytical model

To improve the model, the airgap needed to be more accurately modeled. Note that, the effect of linear part is ignored in part 3.1.

For modeling the non-homogeneous flux distribution throughout the core, it is needed to divide the core into smaller equivalent reluctance paths and calculate them separately. Moreover, some critical airgap sections, such as sharp corners, can also be added to the calculation. The model can be improved by dividing the core and its environment to smaller sections and calculate them separately, which is the point where we use FEA tools.

In the analytical calculations, the core flux distribution is assumed to be uniform. Since in the real core is not infinitely permeable, the inductance may decrease. On the other hand, due to the fringing fluxes and non-homogeneous flux distribution inside the core, the resultant inductance may increase, assuming core did not saturate.

## 4. Question 2: FEA Modeling (2D - Linear Materials)

### 4.1. Flux density distributions at rotor angle 0° - 45° - 90°

In this section, the FEA model of the machine is made using ANSYS Maxwell FEA tool. As material, iron with relative permeability 4000 has chosen. The resultant flux vectors and flux density distributions are provided in Figure 5.

It is clear to see that the flux distribution is not uniform for all cases. The flux always tries to go from the lowest reluctance path, therefore these flux distributions occur. At 0°, the system has the highest inductance and the lowest inductance. Therefore, maximum flux flows when to rotor is in this position. Flux vectors are going in radial direction in the airgap, as can be seen from the Figure 5 flux vector distribution, since it is shortest reluctance path. The flux distribution on the rotary part is symmetrical, meaning that the rotor is at one of its stable positions, meaning that, net torque at this position is ideally zero. Also, the flux is concentrated on the corners and sharp edges of the rotating parts. The core is more likely to saturate at these regions.

At 45°, the inductance is reduced as well as the flux flowing through the core. In this position, it is clearer to see the flux density increment at the sharp edges of rotor part.

At 90°, the flux is at minimum since the rotor at its minimum inductance point. Flux distribution on the rotary part is symmetrical, therefore this position also one of the stable positions.

### 4.2. Inductance and stored energy at rotor angle 0° - 45° - 90°

Inductance and stored energy results are given in Table 1. It can be seen that at 0°, the magnetic energy stored in the core is the highest since the inductance is also at maximum value. Volume integral energy storage and inductance energy are resulted approximately the same value. The FEA calculated inductance values are close to the analytical calculation finding. The results of both methods are compared more intensively in 4.3.

*Table 1: Inductance and stored energy FEA results for linear material*

Rotor angle	Inductance (mH)	Stored Energy (J) (Volume integral)	Stored Energy (J) ( $0.5 \cdot I_{dc}^2 \cdot L$ )
0°	27.29	0.123	0.123
45°	17.53	0.0789	0.0789
90°	8.36	0.0376	0.0376

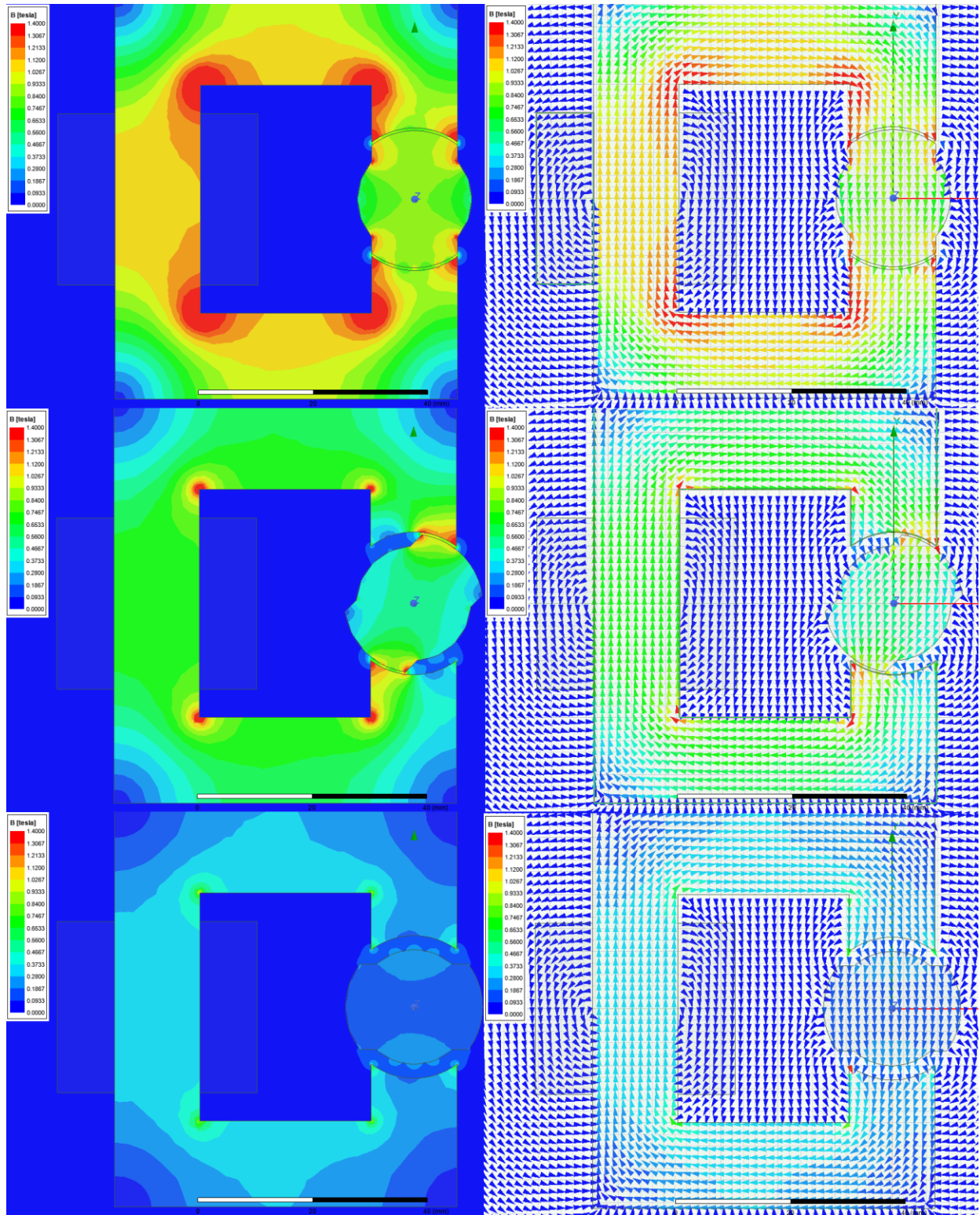


Figure 5: Flux distributions at angle 0°, 45° and 90° degrees for linear material core with relative permeability 4000



#### 4.3. Analytical results and FEA results comparison

To calculate torque values analytically, the change of inductance as a function of rotor angle is taken. Note that, analytical calculation of reluctance, and therefore inductance, is provided in 3.1. Comparison of analytical results and FEA results are provided in Figure 6. The effect of assumptions made in 3.1. can be seen from the figure. The omitted linear part, leakage flux, non-homogeneous flux distribution may have contributed to the difference in the inductance. Moreover, it can be seen that the inductance changes more smoothly when compared to analytical result. Even so, both results look similar to each other. FEA results must be more accurate since the calculation is done over more small pieces. However, analytical results seems to verify the FEA results.

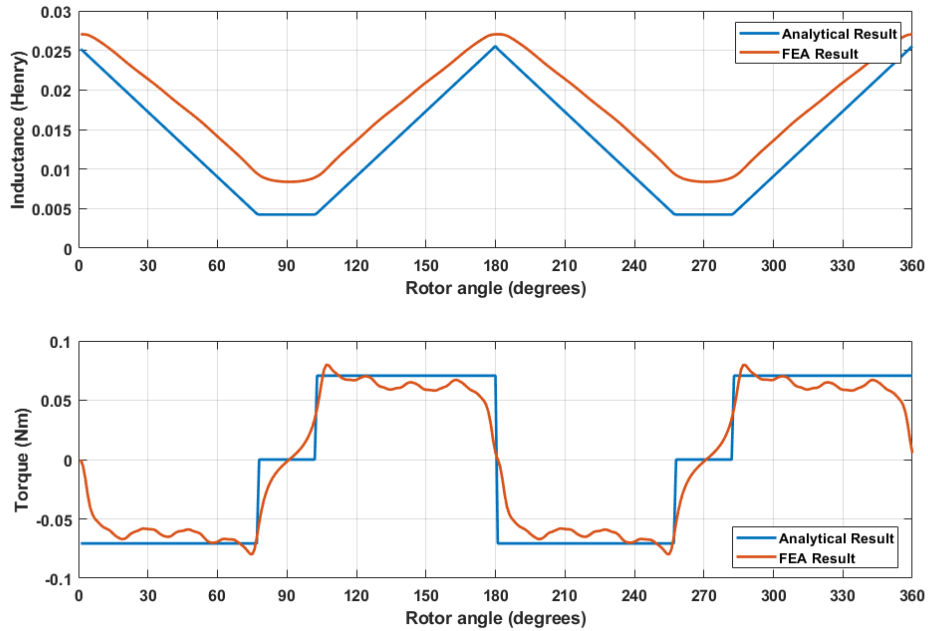


Figure 6: Analytical results and FEA results (linear material) for inductance and torque

## 5. Question 3: FEA Modeling (2D - Nonlinear Materials)

### 5.1. Flux density distributions at rotor angle $0^\circ$ - $45^\circ$ - $90^\circ$

In this section, a material named as M19\_26G is used for analysis. The B-H curve of the material is provided in Figure 6.

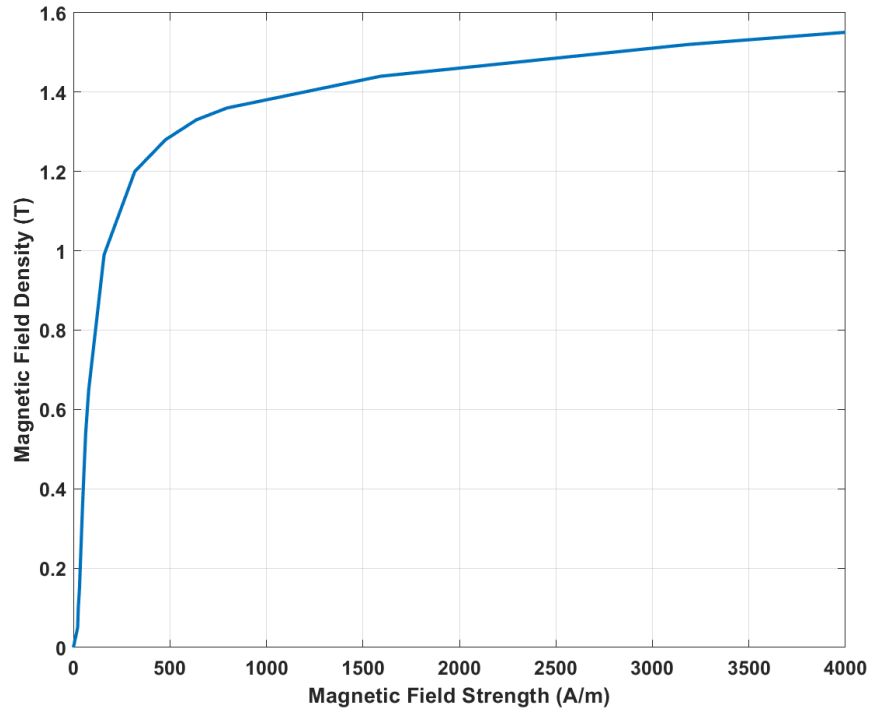


Figure 7: M19\_26G material B-H curve

Flux density distribution and flux density vector distribution of the material is provided in Figure 8, whereas the comparison of flux density vectors of linear and nonlinear materials is provided in Figure 9.

It can be seen from figure 9 that the flux is more distributed on the core with linear material. The reason is that since the material saturates above some flux density value, the flux tries to flow through more non-saturated (i.e. low reluctance) paths. Moreover, the saturation effect reduces the overall red areas on the flux density graph, since as flux density increases equivalent reluctance of the material increases. Above some flux density value, the core's relative permeability is close to that of air.

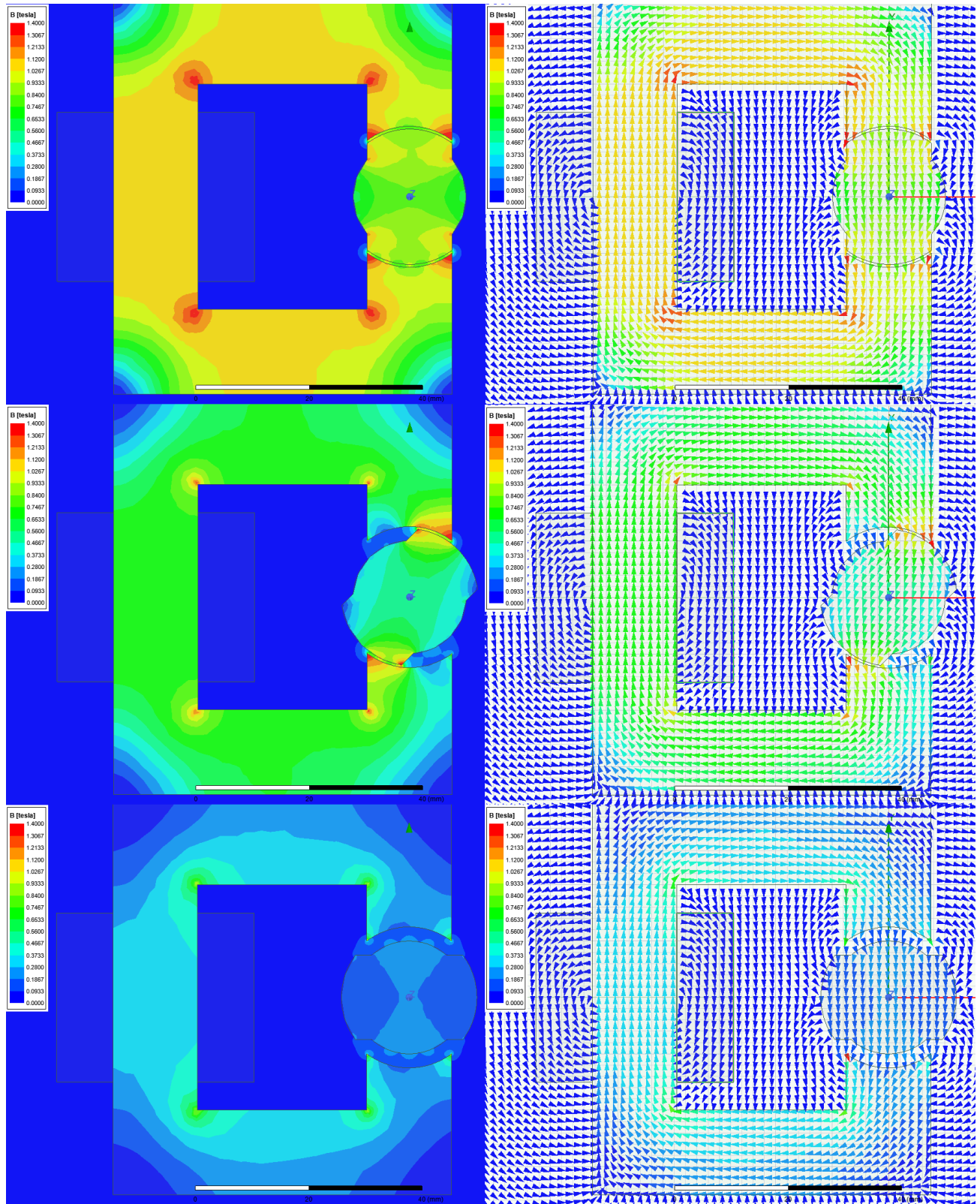


Figure 8: Flux distributions at angle 0°, 45° and 90° degrees for M19\_26G (nonlinear material)

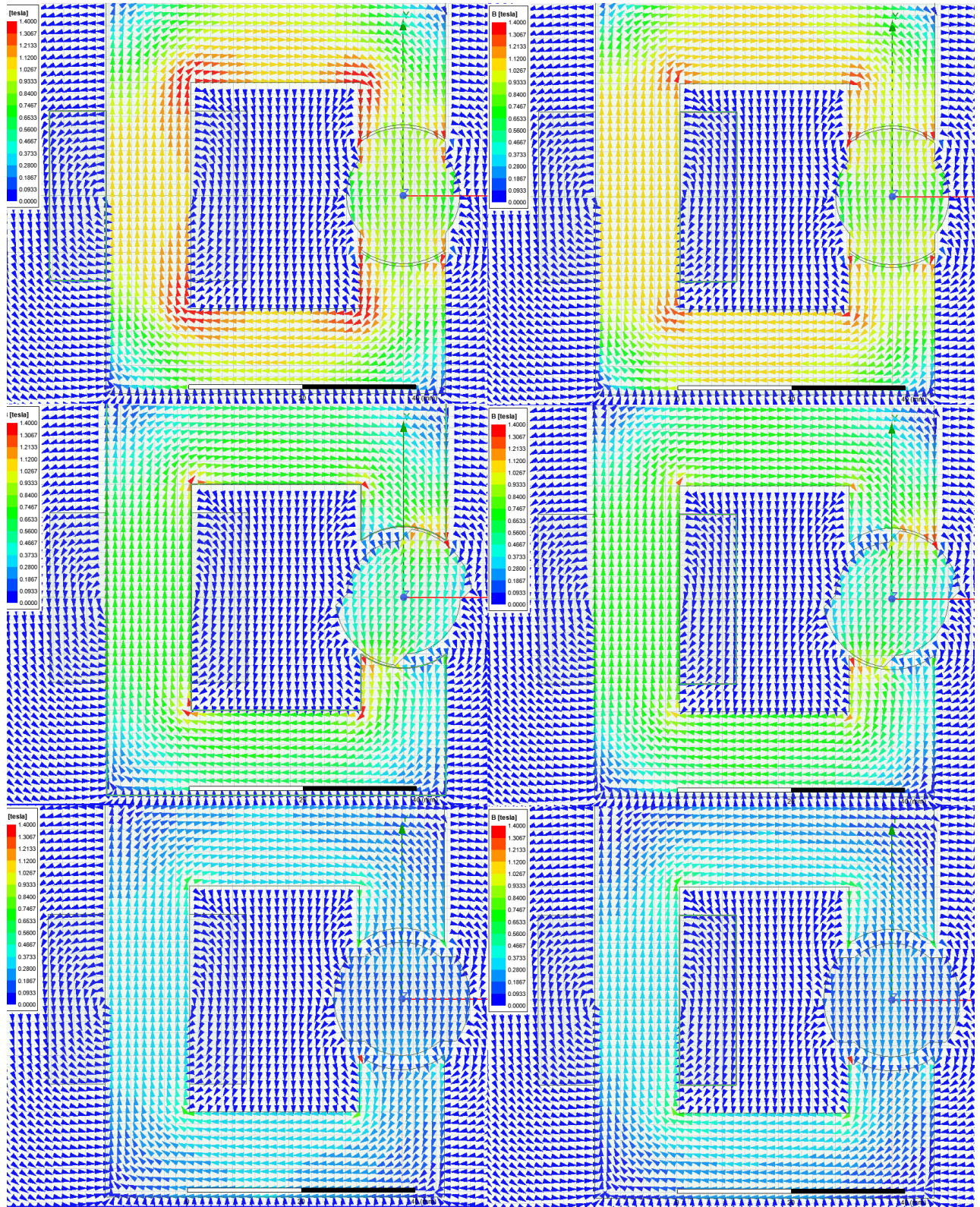


Figure 9: Flux density vector comparison of linear material in Question 2 (on the left) and nonlinear material in Question 3 (on the right) at angle  $0^\circ$ ,  $45^\circ$  and  $90^\circ$  degrees



## 5.2. Inductance and stored energy at rotor angle 0° - 45° - 90°

Inductance and stored energy results for nonlinear material are given in Table 2. When compared to the linear material, the overall inductance has changed just slightly and the calculated stored energies seem close to each other. Since there is no saturation, the effect of having a nonlinear material is not very significant.

Table 2: Inductance and stored energy FEA results for nonlinear material

Rotor angle	Inductance (mH)	Stored Energy (J) (Volume integral)	Stored Energy (J) ( $0.5 \cdot I_{dc}^2 \cdot L$ )
0°	27.00	0.1197	0.121
45°	17.619	0.07916	0.0793
90°	8.38	0.0378	0.0377

## 5.3. Analytical results and FEA results comparison

FEA results for linear and nonlinear materials are provided in Figure 10. The similarity in inductance and energy storage values resulted in similar torque and inductance values for both materials.

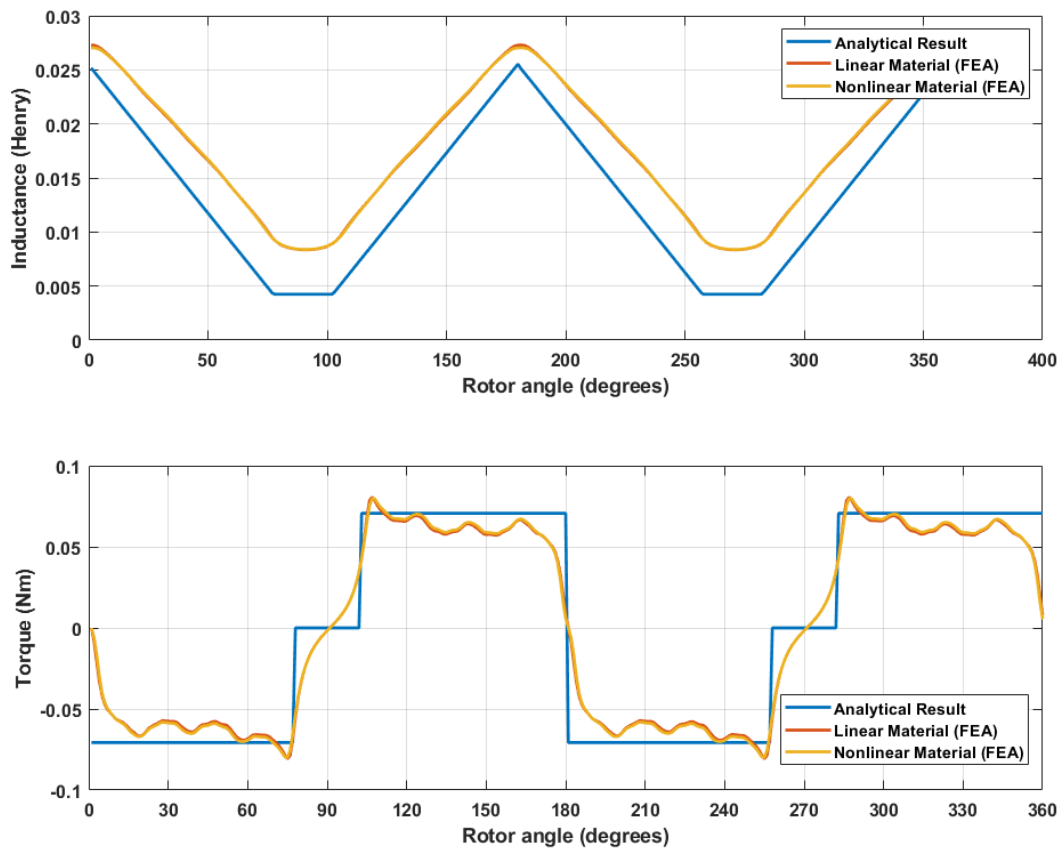


Figure 10: Analytical results and FEA results for linear (M19\_26G) and nonlinear material for inductance and torque

## 6. Question 4: Control Method

In this machine, since there is no excitation and/or permanent magnet on rotor, only torque component is the reluctance torque. As can be seen from Figure 6 & 10, in order to produce a torque whose mean value is non-zero, the excitation to the coils should be given at certain angles of the rotors.

To obtain a rotation in positive direction, the coils of the machine should be excited with DC current when the position of the rotor is between  $90^\circ$ - $180^\circ$  and  $270^\circ$ - $360^\circ$ , since between these angles the torque on the rotor is positive. Note that the direction of the excitation current is independent of the direction of the torque produced on the rotor.

To obtain a rotation in negative direction, the coils of the machine should be excited with DC current when the position of the rotor is between  $0^\circ$ - $90^\circ$  and  $180^\circ$ - $270^\circ$ , since between these angles the torque on the rotor is negative. Note that the direction of the excitation current is independent of the direction of the torque produced on the rotor.

## 7. Question 5: Motion Animation

The change of flux density with the rotor position animation for linear material is provided can be found in [this link](#).

## 8. References

[1] - <https://github.com/odtu/ee568/tree/master/Project1>